



Montréal, Québec
May 29 to June 1, 2013 / 29 mai au 1 juin 2013

High performance ECC floor slabs in coupled shear wall structures

Rizwan Issani and Khandaker M.A. Hossain

Department of Civil Engineering, Ryerson University, Toronto, Ontario, Canada

Abstract: Coupled shear wall buildings are popular form of high rise structures. Flexural behaviour of floor slab acting as coupling beam is very important for the analysis of such structures. Recent advancement in the new generation of high performance concrete materials provides an alternative to conventional concrete to enhance the performance of coupling slabs. This paper presents the flexural behaviour of coupling slabs incorporating engineered cementitious composite (ECC) as an alternative to conventional concrete. ECC is a unique type of fibre reinforced cementitious materials with ultra high ductility. The high strain capacity while maintaining low crack widths makes ECC an ideal material for the coupling slab application. The non-linear coupling action of ECC link slabs is investigated experimentally with small-scale model specimens under monotonic loading. The ECC coupling slab performance is compared with conventional self-consolidating concrete (SCC) based on load-displacement/moment-rotation response, flexural stiffness, deflection capacity enhancement, crack control characteristics and failure modes.

1. Introduction

Coupled shear wall (CSW) structures are popular form of high rise structures where shear walls are directly connected to floor slabs (Hossain 2003, Coull and Choudhury 1967). Figure 1 shows a coupled shear wall building where two rows of apartments are connected by a common corridor and the partition walls are treated as shear walls. The structural analysis and design of a slab-coupled shear wall system can be performed using existing techniques of beam coupled shear wall structures, provided that the structural stiffness of the slab which acts as wide coupling beam is known (Rosman 1964, Tso and Mahmoud 1977, Coull and Wong 1990, Hossain 2003).

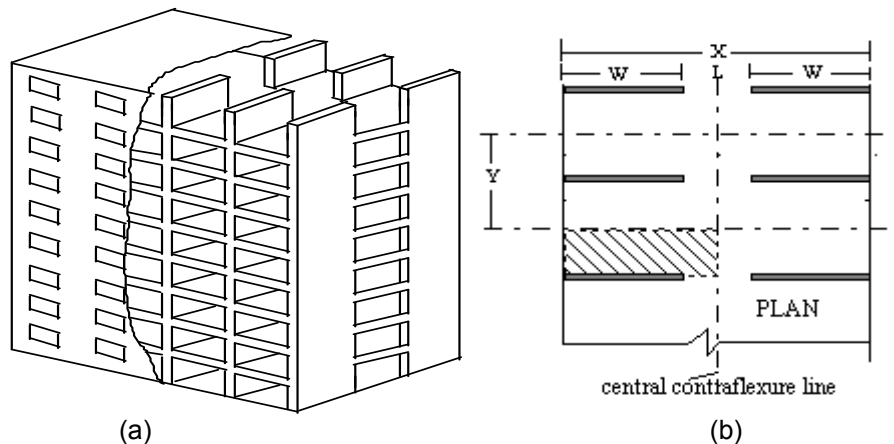


Figure 1: (a) Schematic view with structural components (b) layout plan of coupled shear wall structure

As no projecting system of beams run across the corridor, there is no need for false ceilings and the height of the building is appreciably reduced thus accommodating more floors in the same height of the building. In the plan view of coupled shear wall (Fig. 1b), the two walls of width 'W' having a corridor opening of width 'L' between them are placed symmetrically along the width of the building 'X'. The centre to centre distance between rows of shear walls are denoted by 'Y'.

Coupled shear wall resists lateral loads by cantilever bending action, which results in rotation (Θ) of the wall cross-sections (Fig. 2). The free bending of a pair of shear wall is resisted by the floor slabs, which are forced to rotate and bend out of plane where they are connected rigidly to the walls (Coull and Wong 1990, Hossain 2003). Due to large width of the wall, considerable differential shearing action is imposed on the connecting slab, which develops transverse reactions to resist the wall deformations and induces axial tensile and compressive forces (Q) into the walls (Fig. 2). Due to large lever arm involved, relatively small axial forces can give rise to substantial moment of resistance (M), thereby reducing greatly the wind moments in the walls. Therefore, the lateral stiffness of the structure is increased (Coull and Wong 1990).

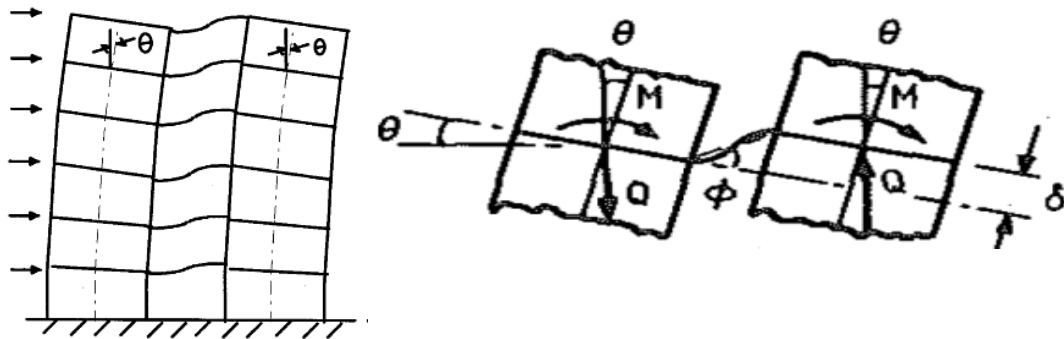


Figure 2: Structural action of CSW building under lateral load

Similarly, the bending of the coupling slab can also be caused by vertical deformation (δ) due to seismic reaction and foundation settlement of the structure as described in Fig. 2 resulting in moment (M), rotation (Θ) and axial tensile/compressive forces (Q) into the walls.

Over the last years, new generation of high performance concrete (HPC) such as Self-Consolidating Concrete (SCC) and Engineered Cementitious Composites (ECCs) with improved strength, durability, ductility and energy absorbing capacity has been developed. SCC is flowable, achieves good consolidation, and can flow into place between congested reinforcement without vibration and without defects due to bleeding or segregation (Khayat 1999, Lachemi et al. 2003, Hossain and Lachemi 2010).

Self-consolidating ECC was also reported to have superior workability, ductility and durability, which translates to speedy construction, reduced maintenance and a longer life span for the structure (Li and Kanda 1998; Wang and Li 2003, Wang and Li 2006, Şahmaran et al. 2009). Micromechanical design allows optimization of ECC for high performance, resulting in extreme tensile strain capacity while minimizing the amount of reinforcing fibres, typically less than 2% by volume. Unlike ordinary cement-based materials, ECC strain hardens after first cracking and demonstrates a strain capacity 300 to 500 times greater than normal concrete through the use of incorporating fibers. Even at large imposed deformation, crack widths of ECC remain small, less than $60 \mu\text{m}$.

The use of HPCs in CSW system can significantly improve the performance in construction and service stages. Self-consolidation properties of SCC and ECC will help pour concrete with ease without consolidation into the heavily reinforced walls and slab components and ensure concrete quality. The knowledge of the behaviour of CSW systems incorporating such new generation of HPCs is very important for implementation of this new HPC technology to construct high rise buildings.

For decades, comprehensive research has been conducted on the ordinary reinforced concrete based CSW system (Coull and Choudhury 1967, Coull Wong 1990, Hossain 2003). To the author's knowledge,

no research has been conducted on coupled shear wall system with Reinforced Engineered Cementitious Composites (RECC) to date. The innovative technology of RECC based CSW system can significantly improve the performance in terms of strength, stiffness, ductility, energy absorbing capacity and durability. Design specifications are also not available in current Codes and existing analysis techniques to accommodate the high strain hardening capacity of ECC and its effect on stresses and deflection characteristics of CSW system.

This paper presents bending/flexural performance of ECC coupling slabs in the shear wall structures by testing small scale model specimens under monotonic loading. The performance study of ECC coupling slab compared with its conventional concrete (SCC) counterpart is presented based on load-deflection response, moment-rotation response, flexural stiffness, ductility enhancement, cracking pattern and failure modes.

2. Experimental Investigation

A systematic experimental investigation was conducted on the non-linear behaviour of reinforced ECC and SCC slabs in CSW structures. The CSW model specimens with different configurations with planar shear walls were used. The CSW models were divided into three different groups having L/X of 0.3, 0.4 and 0.6 with Y/X of 0.1 having constant reinforcement in the slab. The tests provided information on load-deflection ($Q-\delta$) response, stress-strain development in steel and concrete and failure modes including cracking and crack propagation.

2.1 Simulation of Flexural Behaviour of Coupling Slab and Working Principle of Test Set-up

A schematic of the experimental set-up and its working principle are presented in the Fig. 3. One leg (wall) of the test model is fixed to the fixed platform through base plate-fixing angle assembly while the other leg was fixed in a similar manner to the movable/free platform. Upward load (Q), was then applied through hydraulic actuator at the movable end and corresponding vertical deflection (δ), of the platform was monitored. The load (Q), was applied through the centre of the wall incrementally until failure of the slab to get complete $Q-\delta$ and hence, moment-rotation ($M-\theta$) responses as shown in Fig. 3. The model tests provided information on the strength, stiffness and modes of failure of the system. From $Q-\delta$ and $M-\theta$ responses, the behaviour of slab in pre-cracking to post-yielding stages of CSW system was analyzed.

After 28 days of curing, coupled shear wall specimens were attached to the test set-up for testing under monotonic loading to failure. Four different linear variable displacement transducers (LVDTs) were installed to measure the displacements (δ) at four different critical locations such as at the middle of the movable wall, upper edge of movable wall, center of the slab and center of the fixed wall (Fig. 4). Hydraulic actuator, strain gauges and LVDT's were directly connected to the computerized data acquisition to record load, strain and displacement during the loading history until failure.

Load was applied at the rate of 0.05 kN per minute until the failure of the specimens. During the loading history, load, displacements, strains in concrete and reinforcing steel, cracking, crack propagation, and failure modes of the specimens were observed. From the test, load-displacement ($Q-\delta$) and corresponding moment-rotation ($M-\theta$) response were obtained for each of the CSW model specimens.

2.2 Geometry of Model Test Specimens

Small scale model tests of approximately 1/12th scale of CSW building had been carried out to investigate the general behaviour of the system and to study the effect of geometric parameters. The tests had been conducted for a particular value of Y/X (0.6) with L/X of 0.3, 0.4 and 0.6. However, specimens with L/X of 0.3 will be the subject matter of this paper. Two high performance concretes namely SCC and ECC were used to make the specimens. Detailed dimensions of the models and geometric ratios (L/X and Y/X) are presented in Table 1. The model specimens are designated as 'ECC300' and 'SCC300'. The letters in the model designation represents type of HPC and numerics represent the width of the wall in mm. All geometric dimensions of the model specimens are presented in Fig. 5.

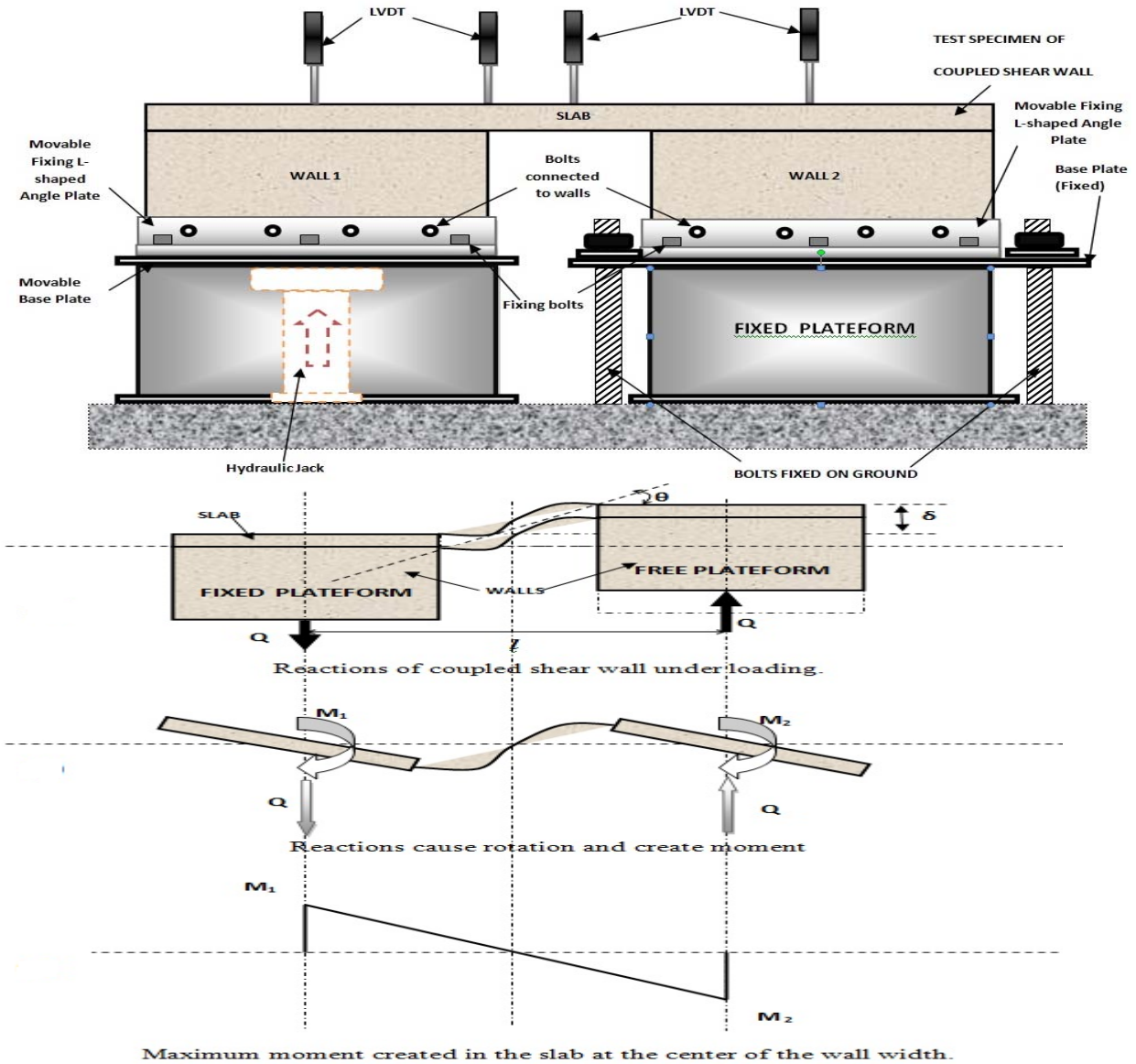


Figure 3: Working principle of test-set-up and behaviour of coupling slab

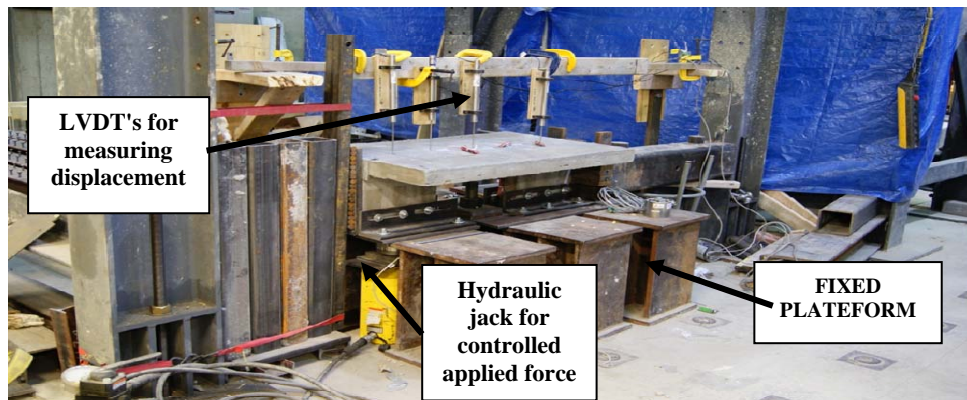


Figure 4: Laboratory test setup (instrumentation)

Table 1: Geometrical parameters of model test specimens

Model	Y/X	L/X	Length of Slab (X) (mm)	Width of the slab (Y) (mm)	Width of the wall (W) (mm)	Thickness of slab (t) (mm)	Wall thickness (t_w) (mm)	Corridor Opening (L) (mm)
ECC300		0.4	1000	600	300	60	75	400
SCC300		0.4	1000	600	300	60	75	400

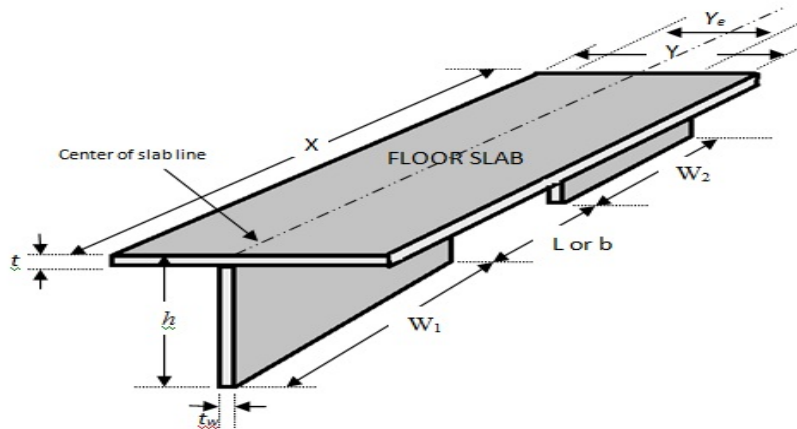


Figure 5: Coupled shear wall model showing geometric parameters

2.3 Material Properties and HPC Mix Designs

The mix designs and ingredients of SCC and ECC are shown in Table 2. Type 10 Portland cement (ASTM Type I), type “S” slag cement, coarse aggregate with maximum size of 8 to 10 mm, well graded sand, and High Range Water Reducing admixtures (HRWRA) were used to make SCC. ECC was made of Type 10 Portland cement (ASTM Type I), Class F fly ash, Polyvinyl Alcohol (PVA) fiber of 8 mm length, HRWRA and silica sand with 110 μm average grain size.

Table 1: Mixture proportions of SCC and ECC

SCC ingredients, kg/m^3					
Cement	Slag	Water	Coarse agg	Fine agg.	HRWRA
400	90	172	750	910	1.85
ECC ingredients, kg/m^3					
Cement	Fly Ash	Water	PVA Fiber	Silica Sand	HRWRA
386	847	327	26	435	3.7

The 28-day compressive strength/modulus of elasticity were obtained from 100 mm x 200 mm cylinders while the flexural strength was obtained from four point bending test on 355 x 76 x 50 mm beam specimens as per ASTM Standards. The mean value of compressive strength, tensile strength and modulus of elasticity of SCC were 38 MPa, 3.35 MPa and 32.1 GPa, respectively compared with 36 MPa, 7.20 MPa and 24.7 GPa, respectively of ECC. The yield strength, ultimate strength and modulus of elasticity of 4.75 mm mild steel bars as determined from coupon specimens were 457 MPa, 525 MPa and 153 GPa, respectively.

2.4 Design of Models and Reinforcement Details

Small-scale model specimens used in this study were similar to those used by Hossain (2003) where the reinforcements were calculated based on an equivalent static uniform wind load of 8.76 kN/m along the height of the building. The maximum wind shear, induced in the most highly stressed slab of a 20-storied coupled shear wall building having storey height of 3m and slab thickness of 200 mm, was calculated by using continuous medium method (Coull and Choudhury 1967, Hossain 2003). The slab was then designed for reinforcement by applying maximum wind shear along the central contra-flexure line (Fig. 1b). In model specimens, reinforcements in the form of mesh of 100 mm x 100 mm in size were provided as shown in Fig. 6. Wall reinforcements were also provided in the form of mesh (50 mm x 50 mm) in the same manner. Walls were highly reinforced with two layers of the same size mesh. Reinforcements were extended from walls and coupled with slab reinforcements to give strong wall-slab joints to ensure the failure of slabs before wall and joint.

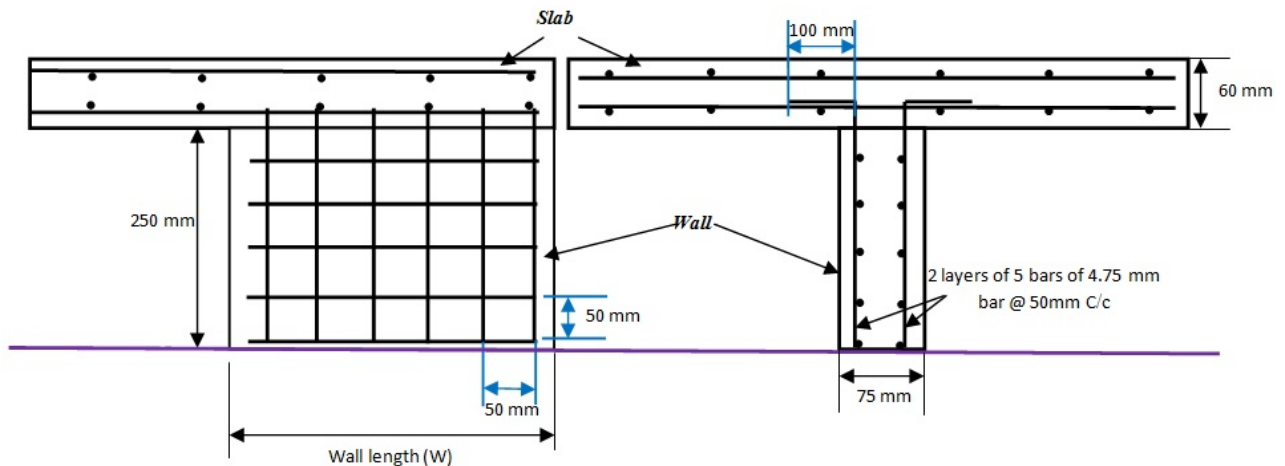


Figure 6: Reinforcements in the CSW specimens

The slab moment capacity (M_r) under flexure was derived according to CSA A23.3-04 (2009). The analytical equivalent storey shear load resistance (Q_a) for the coupling slabs of model specimens was calculated based on the analytical moment resistance (M_r) and considering the critical section at the junction of the interior edge of the shear wall. The analytical storey shear load resistance of ECC and SCC model specimens are presented in Table 3.

Table 3: Analytical moment and shear load resistance of coupling slab

Model	Ultimate equivalent storey shear load capacity of coupling slab (kN)		
	Analytical (CSA A23.3-04,2009)	Experimental	Ratio
	$Q_a = 2M_r/L$	Q_{exp}	Q_{exp}/Q_a
ECC300	10.77	19.59	1.82
SCC300	10.79	10.94	1.01
M_r : SCC = 2.159 kN.m; ECC = 2.154 kN.m			

2.5 Casting of Model Specimens

The casting of specimens was carried out in the Concrete Laboratory of Ryerson University. A flexible wooden mould was designed and fabricated as shown in Fig. 7. Immediately after mixing, ECC/SCC was poured into the mould without consolidation. Fig. 7 also shows the typical casting of ECC specimen. Highly flowable ECC went inside the narrow gaps of heavily reinforced walls with ease saving construction time and ensuring high quality work without voids. Same ease of casting was observed with

flowable SCC. Control specimens in the form of cylinders and beams were also cast at the same time. After casting, CSW model and control specimens were covered with plastic sheets. After 48 hours, model and control specimens were de-moulded. Model and control specimens (covered with plastic bags) were then left to air cure under uncontrolled conditions of humidity and temperature until testing at the age of 28 days.



Figure 7: Casting of highly flowable ECC mixture into the mould

3. Results and Discussions

3.1 Strain Development in Coupling Slab

The strain gauges were installed at key locations in the reinforcing bars before casting of concrete and also on the concrete surface as shown in Fig. 8. All the strain gauges were located along the centre line of the slab in line with the walls.

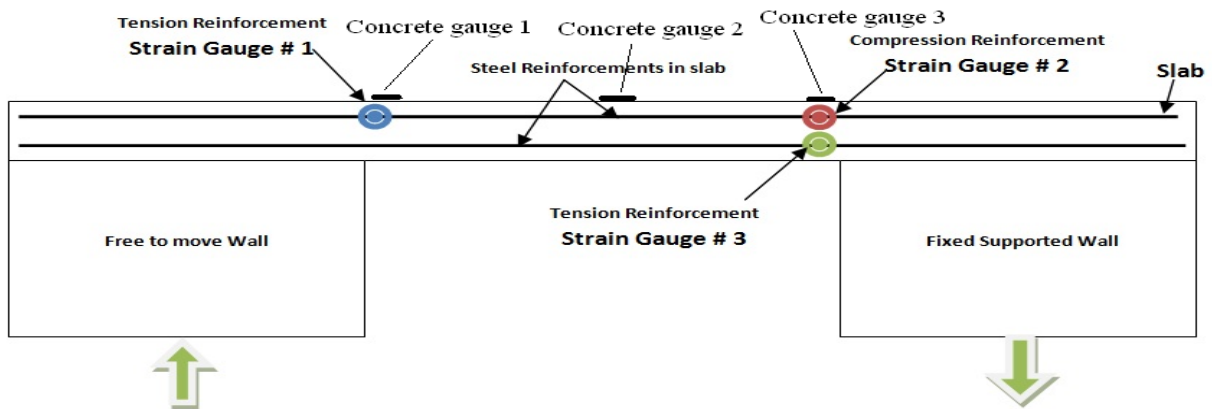


Figure 8: Locations of strain gauges at slab reinforcements and concrete

Figure 9 shows a typical load-steel strain response. It is noted that steel at the tension (strain gauges 1 and 3) zone yielded before failure. The strain development in strain gauge 2 confirms that the steel in the compression zone was not yielded even the slab reached its ultimate load carrying capacity. For all the specimens, failure was due to the failure of coupling slab along a transverse line passing through the edge of the shear wall where reinforcements were yielded.

Fig. 10 compares the load-concrete strain responses of SCC and ECC model specimens. It is interesting to note that ECC slabs developed significantly higher tensile and compressive strain compared to their SCC counterparts. This can be associated with the higher strain hardening capacity of ECC and its capability to produce micro-cracking. This signifies the superior performance of ECC slabs compared to SCC slabs in terms of ductility and energy absorbing capacity of the system.

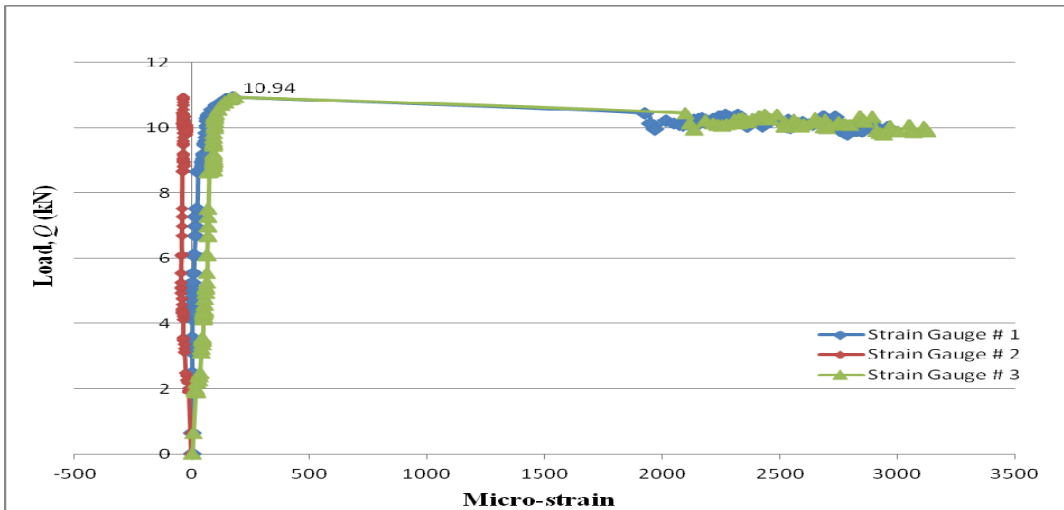


Figure 9: Load-steel strain response

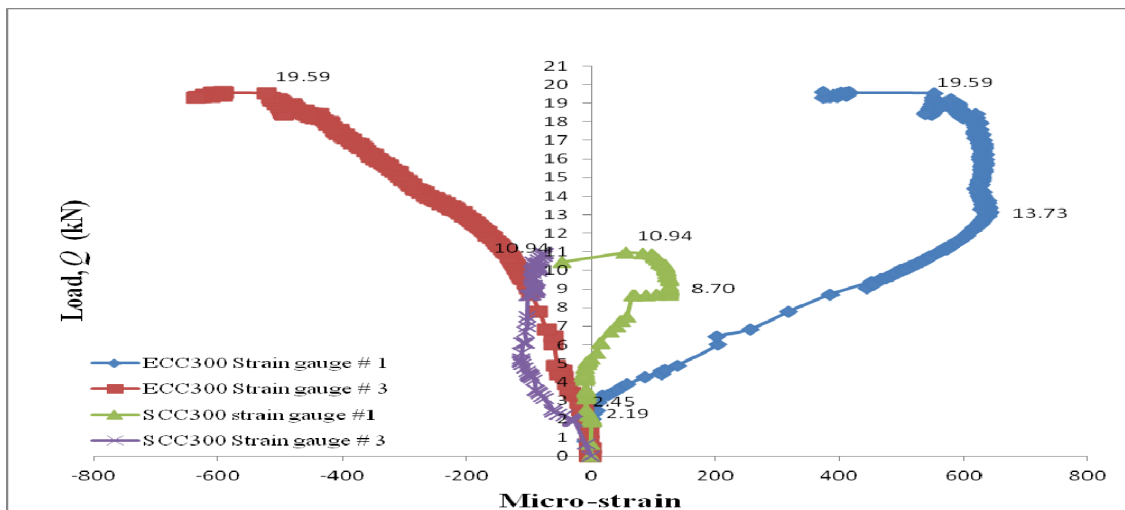


Figure 10: Comparison of load-concrete strain relationship of ECC and SCC

3.2 Load-Displacement/Moment-Rotation Response, Crack Development and Failure Modes

Experimental load-displacement ($Q-\delta$)/moment-rotation ($M-\theta$) responses of CSW model specimens are analyzed to compare the performance ECC and SCC based on strength and ductility point of view. Table 4 summarizes cracking, yielding and ultimate loads and corresponding displacement of the CSW specimens.

Table 4: Summary load-displacement response and ductility of CSW models

	Load (Q) (kN)			Displacement (δ) (mm)			Ratio	
	Cracking	Yielding	Ultimate (Peak)	Cracking	Yielding	Ultimate (Peak)	${}^+Q_{uECC}/Q_{uSCC}$	${}^*\delta_{uECC}/\delta_{uECC} = \psi$
ECC	2.45	13.12	19.59	0.53	8.46	14.80	1.79	1.32
SCC	2.19	9.25	10.94	0.42	6.45	11.17		

${}^+Q_{uECC}/Q_{uSCC}$ = Ratio of ultimate load ψ : Relative ductility

ECC specimens developed very fine and large number micro-cracks in contrast to the development of one or two major cracks with large crack width in SCC specimens (Fig. 11).

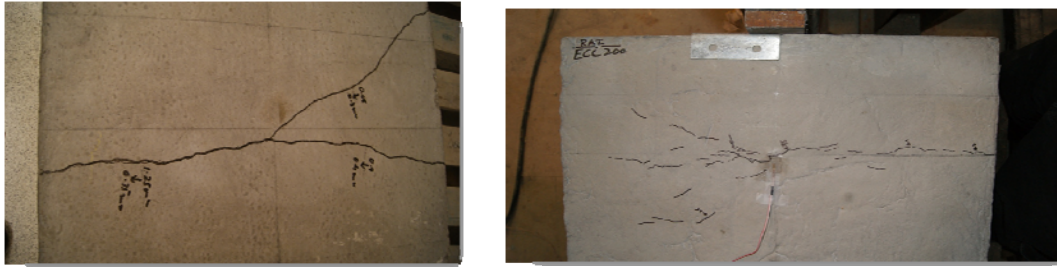


Figure 11: Crack development in SCC and ECC specimens at the inner edges of the wall

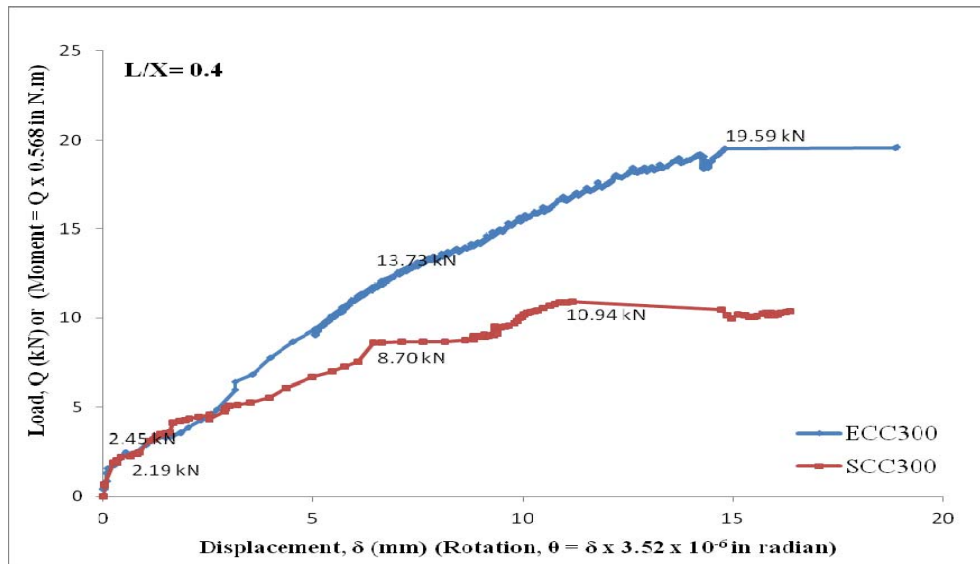


Figure 12: Experimental load-displacement/moment-rotation responses of ECC and SCC specimens

Fig. 12 compares the load-displacement/moment-rotation responses of SCC and ECC specimens. In ECC specimens cracking started at 2.45 kN around 12.51% of the ultimate load and in SCC at 2.19 kN around 20.02% of the ultimate load (Table 4). Yielding of steel in ECC started at 70.09% of ultimate load and in SCC300 at 79.52% of ultimate load. Ultimately, ECC specimens failed at much higher load of 19.51 kN compared to 10.1 kN of their SCC counterparts. ECC specimen showed 10.61% and 20.75% higher load and displacement, respectively at cracking, 36.64% and 23.76% higher load and displacement respectively at yielding and 44.16% and 24.53% higher load and displacement respectively at failure compared with its SCC counterpart. ECC specimen showed 1.32 times more ductility and 1.79 times higher ultimate load compared to its SCC counterpart (Table 4). The bigger load-displacement envelope also shows higher energy absorbing capacity of ECC CSW specimens compared to their SCC counterparts.

3.3 Comparison of Experimental and Theoretical Load Capacity

Table 3 compares theoretical load capacity of SCC/ECC coupling slab based on CSA A23.3-04 (2009) with those obtained from model tests. CSA A23.3-04 (2009) seems to have predicted load capacity of SCC coupling slabs reasonably well with the ratio of experimental to theoretical/Code predicated values of 1.01. On the other hand, CSA A23.3-04 under predicted load capacity of ECC coupling slabs with the ratio of experimental to theoretical/Code predicated values of 1.79. Higher load capacity of ECC coupling slab is attributed to the presence of PVA fibers acting as reinforcement whose contributions to load carrying capacity are not considered in the CSA A23.3-04 (2009) Code. Presence of PVA fibers significantly improved the crack resistance of ECC by bridging cracks and inducing lower stress transfer to embedded reinforcement (which delayed the yielding of steel) and hence, significantly improved post-

cracking and post-yielding load resistance of ECC slabs. This is evident from the long cracking to post-yielding branch of the load-displacement responses of ECC slab showing significant strain hardening compared with SCC (Fig. 12).

4. Conclusions

The following conclusions are drawn from this study:

- ECC coupling slabs have developed significantly higher tensile/compressive strain compared to their SCC counterparts. All model CSW specimens have failed due to the failure of coupling slabs along a transverse line passing through the interior edge of the shear wall where tension reinforcements are yielded. Failure of the ECC specimens is characterized by the formation large number of very fine micro-cracks compared to one or two major cracks (with large crack width) in SCC specimens.
- Cracking, yielding and ultimate loads are higher for ECC specimens compared to SCC specimens. ECC slabs exhibits more ductility and higher ultimate load compared to their SCC counterparts. The bigger load-displacement/moment-rotation envelop also demonstrates higher energy absorbing capacity of ECC CSW specimens compared to their SCC counterparts.
- Canadian Code (CSA A23.3-04, 2009) has predicted load capacity of SCC coupling slabs reasonably well with a mean ratio of experimental to theoretical/Code predicated load of 1.10. On the other hand, (CSA A23.3-04, 2009) under-predicts load capacity of ECC coupling slabs with a mean ratio of experimental to theoretical/Code predicated load of 2.06.

This research confirms the viability of constructing reinforced ECC coupled shear wall building with enhanced strength, ductility and energy absorbing caapcity. Use of such shear wall system will be highly effective for high rise buildings located in areas with high seismic risk.

References

- CSA Standard A23.3-04 (2009). "Concrete Design Handbook." *Canadian Portland Cements Association Handbook, 2nd edition, Canada.*
- Coull, A. and Choudhury, J.R. (1967). "Analysis of Coupled Shear Walls." *Proc. ACI Journal*, 64(9), 587-593.
- Coull, A. and Wong, Y.C. (1990). "Cracked Coupling Slabs in Shear Wall Buildings." *Proc. Journal of Structural Engineering, ASCE*, 116(6), 1744-1748.
- Hossain, K. M. A. (2003). "Non-linear Performance of Slabs in Coupled Shear Wall Structures." *Advances in Structural Engineering- An International Journal*, 6(4), 341-354.
- Hossain, K.M.A. and Lachemi M. (2010). "Fresh, Mechanical, and Durability Characteristics of Self-Consolidating Concrete Incorporating Volcanic Ash." *Journal of Materials in Civil Engineering, ASCE*, 22(7), 651-657.
- Khayat, K.H. (1999). "Workability, Testing, and Performance of Self-Consolidating Concrete." *ACI Materials Journal*, 96(3), 346–353.
- Lachemi, M., Hossain, K.M.A., Lambros, V. and Bouzoubaâ, N. (2003). "Development of Cost-Effective Self-Consolidating Concrete Incorporating Fly Ash, Slag Cement, or Viscosity-Modifying Admixtures." *ACI Materials Journal*, 100(5), 419–425.
- Rosman, R., (1964). "Approximate Analysis of Shear Walls Subjected to Lateral Load." *Proc., ACI Journal*, 61(6), 717-734.
- Şahmaran, M., Lachemi, M., Hossain, K.M.A. and Li, V.C. (2009). "Influence of Aggregate Type and Size on the Ductility and Mechanical Properties of ECC." *ACI Materials Journal*, 106(3), 308-316.
- Tso, W.K., and Mahmoud, M.A. (1977). "Effective Width of Coupling Slabs in Shear Wall Buildings." *Journal of Structural Division. ASCE*, 103(3), 573-586.
- Wang, S. and Li, V. C. (2003). "Materials Design of Lightweight PVA-ECC." *Proc. of the 4th International RILEM Workshop on High-Performance Fiber-Reinforced Cement Composites (HPFRCC 4)*, Naaman, A. E. and Reinhardt, H. W., Eds., RILEM, Paris, 379 –390.
- Wang, S. and Li, V.C. (2006). "High-Early-Strength Engineered Cementitious Composites." *ACI Materials Journal*, 103(2), 97-105.